Molecular Orbital Studies of Titanium Nitride Chemical Vapor Deposition: Gas Phase Complex Formation, Ligand Exchange, and Elimination Reactions

Jason B. Cross and H. Bernhard Schlegel*

Department of Chemistry, Wayne State University, Detroit, Michigan, 48202

Received February 8, 2000. Revised Manuscript Received June 6, 2000

The chemical vapor deposition (CVD) of titanium nitride can be carried out with $TiCl_4$ or $Ti(NR_2)_4$ and NH_3. The present study uses molecular orbital methods to examine complexes of NH_3 with $TiCl_4$ and $Ti(NH_2)_4$ and the subsequent reaction paths for ligand exchange and elimination reactions which may occur in the gas phase. Geometry optimizations were carried out at the B3LYP/6-311G(d) level of density functional theory, and energies were calculated using a variety of levels of theory, up to G2 for systems with five or fewer heavy atoms. The $TiCl_4{\cdot}NH_3$, $TiCl_4{\cdot}(NH_3)_2$, and $Ti(NH_2)_4{\cdot}NH_3$ complexes are bound by 14.9, 30.9, and 7.9 kcal/mol, respectively. The barrier for $TiCl_4 + NH_3 \rightarrow TiCl_3NH_2 + HCl$ is 18.4 kcal/mol and is lowered by 23.1 kcal/mol with the introduction of a second NH_3. The computed barrier height of 8.4 kcal/mol for the $Ti(NH_2)_4 + NH_3$ ligand exchange reaction is in very good agreement with the experimental activation energy of 8 kcal/mol for $Ti(NMe_2)_4 + NH_3$ ligand exchange. The barrier for formation of $Ti(NH_2)_2NH$ by elimination from $Ti(NH_2)_4$ is 33.5 kcal/mol and is reduced by 10 kcal/mol when assisted by an additional NH_3. However, examination of the free energies at CVD conditions indicates that the reactions without catalysis by an extra NH_3 are favored. Further elimination of NH_3 from $Ti(NH_2)_2NH$ can yield a diimido product, $Ti(NH)_2$, or a nitrido product, $Ti(NH_2)N$, but the barriers and heats of reaction are sufficiently high to make these reactions unlikely in the gas phase during the CVD process.

Introduction

Titanium nitride thin films have a variety of properties, such as extreme hardness, high chemical resistivity, good electrical conductivity, and optical properties similar to gold, which make them useful for a number of industrial and commercial applications, including wear-resistant coatings for tools, barrier materials and conductive coatings for microelectronics, and decorative coatings.[1−3] Chemical vapor deposition (CVD) is the preferred method for preparing thin films for semiconductor applications, because it produces good conformal coatings which are needed for submicron devices.[2] There are a number of methods for preparing Ti−N using CVD.[4−11] One of the primary challenges is to find a suitable low-temperature process for producing films that have the desired properties and are free of impurities.

High-quality Ti−N films can be deposited at high temperatures (900−1000 °C) using $TiCl_4$, N_2, and H_2.[5,6] The temperature can be significantly reduced (500−700 °C) if ammonia is used as the nitrogen source:[7]

$$TiCl_4 + {}^4/_3NH_3 \rightarrow TiN + 4HCl + {}^1/_6N_2 \qquad (1)$$

However, if the temperature is too low, the films contain a mixture of TiN and TiNCl.[8] Ti(IV) amido precursors, $Ti(NR_2)_4$, have been used to avoid chlorine impurities in the thin films.[9,10,12,13] Deposition can then proceed at lower temperatures, but contamination from titanium carbide and organic carbon becomes a problem. Dubois[4,14] has found evidence of Ti−N−C metallocycles that could be the source of the carbon contamination. These impurities can be overcome by using an excess of ammonia, resulting in high-quality films at relatively low temperatures (300−400 °C):[11,15,1615,16]

(1) Buhl, R.; Pulker, H. K.; Moll, E. *Thin Solid Films* **1981**, *80*, 265.
(2) Pintchovski, F.; Travis, E. *Mater. Res. Soc. Symp. Proc.* **1992**, *260*, 777.
(3) Travis, E. O.; Fiordalice, R. W. *Thin Solid Films* **1993**, *236*, 325−329.
(4) Dubois, L. H. *Polyhedron* **1994**, *13*, 1329−1336.
(5) Hoffman, D. M. *Polyhedron* **1994**, *13*, 1169−1179.
(6) Schintlmeister, W.; Pacher, O.; Pfaffinger, K.; Raine, T. *J. Electrochem. Soc.* **1976**, *123*, 924−929.
(7) Kurtz, S. R.; Gordon, R. G. *Thin Solid Flims* **1986**, *140*, 277.
(8) Hegde, R. I.; Fiordalice, R. W.; Tobin, P. J. *Appl. Phys. Lett.* **1993**, *62*, 2326−2328.
(9) Fix, R. M.; Gordon, R. G.; Hoffman, D. M. *Chem. Mater.* **1990**, *2*, 235−241.
(10) Fix, R. M.; Gordon, R. G.; Hoffman, D. M. *Mater. Res. Soc. Symp. Proc.* **1990**, *168*, 357−362.
(11) Fix, R.; Gordon, R. G.; Hoffman, D. M. *Chem. Mater.* **1991**, *3*, 1138−1148.
(12) Sugiyama, K.; Pac, S.; Takahashi, Y.; Motojima, S. *J. Electrochem. Soc.* **1975**, *122*, 614−619.
(13) Fix, R. M.; Gordon, R. G.; Hoffman, D. M. *J. Am. Chem. Soc.* **1990**, *112*, 7833−7835.
(14) Dubois, L. H.; Zegarski, B. R.; Girolami, G. S. *J. Electrochem. Soc.* **1992**, *139*, 3603−3609.
(15) Musher, J. N.; Gordon, R. G. *J. Electrochem. Soc.* **1996**, *143*, 736−744.
(16) Musher, J. N.; Gordon, R. G. *J. Mater. Res.* **1996**, *11*, 989−1001.

10.1021/cm000107l CCC: $19.00
Published on Web 07/21/2000

$$Ti(NR_2)_4 + \text{excess } NH_3 \rightarrow TiN + \text{volatile organics} \quad (2)$$

In low-pressure CVD of TiN films, reactions occur almost exclusively at the surface.[17] However, gas-phase reactions are key components of atmospheric pressure TiN CVD.[5] Through a combination of experimental and computational work, some of the details of this gas-phase chemistry are beginning to emerge. Relatively little is known about the thermochemistry of potential intermediates in Ti−N CVD. To fill this gap, we have calculated the gas-phase heats of formation of $TiCl_m(NH_2)_n$, $TiCl_m(NH_2)_nNH$, and $TiCl_m(NH_2)_nN$ at the G2 level of theory.[18] The results agree well with recent experimental values for $TiCl_n$[19] and should yield theoretical bond dissociation energies accurate to ±2 kcal/mol for the potential intermediates in titanium nitride CVD.

The reaction of NH_3 with Ti complexes appears to be an essential first step for both process 1 and 2. Dubois and co-workers[4,20] have shown that the nitrogen in TiN films produced from amido complexes is derived exclusively from NH_3. Ammonia readily forms complexes with $TiCl_4$ and with $TiCl_2(NR_2)_2$.[21−23] Siodmiak, Frenking, and Korkin[24] have studied ammonolysis of $TiCl_4$ at the B3LYP, MP2, and CCSD(T) levels of theory using pseudopotentials and a split-valence basis set. The binding energy of $TiCl_4 + NH_3$ has been calculated to be ca. 12−24 kcal/mol,[24,25] and the replacement of Cl by NH_2 is computed to be endothermic by 10−20 kcal/mol per Cl.[18,24] Experimentally, the reaction between $Ti(NR_2)_4$ and NH_3 occurs readily,[26−28] and activation energies of 8 and 12 kcal/mol have been measured for R = Me and Et, respectively. This reaction is inhibited by HNR_2 and may be the rate-limiting step when CVD is controlled by gas-phase kinetics.[26−28] Dubois[4] has demonstrated that the hydrogen in HNR_2 comes from the added ammonia.

The next step in the CVD process must be the elimination of either HCl or NH_3 and can happen in the gas phase or on the surface. Gordon and co-workers[9−11] have suggested imido complexes, $TiX_2{=}NH$, may be important gas-phase intermediates. Evidence for this has been provided by Winter and co-workers, who have produced high-quality TiN films using single source titanium amido precursors and have mass spectral evidence of titanium imido complexes as intermediates in the CVD.[23,29] Also, by analyzing the kinetics of CVD, Weiller found that the reversible transamination reaction is followed by an irreversible reaction, most likely an elimination to form an imido complex.[26−28] Dubois[4] has evidence for the formation of large oligiomeric clusters that decompose on the surface. Cundari et al.[30−33] have calculated a number of decomposition reactions of model compounds for CVD intermediates. Using a modest level of theory, they found that reactions forming imido complexes from $TiH_2(NH_2)X$ had barriers of 30−35 kcal/mol for amine elimination and 50 kcal/mol for HCl elimination.

Ultimately, the Ti(IV) in the precursors must be reduced to Ti(III) in the film. Simple bond cleavage in the gas phase can probably be ruled out, since the bond dissociation energies are too high (75−120 kcal/mol calculated for Ti(IV) chloro, amido, imido, and nitrido compounds[18]). No viable gas-phase mechanisms are apparent for other products of reduction such as N_2. Most likely the reduction occurs at the surface, where reactive intermediates and transition states can be more readily stabilized.

In this paper we use computational methods to explore the initial gas-phase reactions of $TiCl_4$ and $Ti(NH_2)_4$ with NH_3 shown in Figures 1 and 2. The more extensive set of reactions examined and the significantly larger basis sets and higher levels of theory used in the present work should provide a more accurate description of gas-phase elimination reactions of the archetypal intermediates $TiCl_3NH_2$ and $Ti(NH_2)_4$. These may also serve as models for nitride CVD processes for early transition metals other than titanium.[5,13,34]

Method

Molecular orbital calculations were carried out using the GAUSSIAN 98[35] series of programs. Equilibrium geometries were optimized by the B3LYP density functional method[36−38] using the 6-311G(d) basis set.[39−43]

(17) Truong, C. M.; Chen, P. J.; Corneille, J. S.; Oh, W. S.; Goodman, D. W. *J. Phys. Chem.* **1995**, *99*, 8831−8842.
(18) Baboul, A. G.; Schlegel, H. B. *J. Phys. Chem. B* **1998**, *102*, 5152−5157.
(19) Hildenbrand, D. L. *High. Temp. Mater. Sci.* **1996**, *35*, 151−158.
(20) Prybyla, J. A.; Chiang, C. M.; Dubois, L. H. *J. Electrochem. Soc.* **1993**, *140*, 2695−2702.
(21) Everhart, J. B.; Ault, B. S. *Inorg. Chem.* **1995**, *34*, 4379−4384.
(22) Winter, C. H.; Lewkebandara, T. S.; Sheridan, P. H.; Proscia, J. W. *Mater. Res. Soc. Symp. Proc.* **1993**, *282*, 293.
(23) Winter, C. H.; Lewkebandara, T. S.; Proscia, J. W.; Rheingold, A. L. *Inorg. Chem.* **1994**, *33*, 1227−1229.
(24) Siodmiak, M.; Frenking, G.; Korkin, A. *J. Mol. Model.* **2000**, *6*, 413−424.
(25) Allendorf, M. D.; Janssen, C. L.; Colvin, M. E.; Melius, C. F.; Nielsen, I. M. B.; Osterheld, T. H.; Ho, P. *Proc. Electrochem. Soc.* **1995**, *95−2*, 393−400.
(26) Weiller, B. H. *Chem. Mater.* **1995**, *7*, 1609−1611.
(27) Weiller, B. H. *J. Am. Chem. Soc.* **1996**, *118*, 4975−4983.
(28) Weiller, B. H. *Mater. Res. Soc. Symp. Proc. ULSI* **1996**, *11*, 409−415.
(29) Winter, C. H.; Sheridan, P. H.; Lewkebandara, T. S.; Heeg, M. J.; Proscia, J. W. *J. Am. Chem. Soc.* **1992**, *114*, 1095−1097.
(30) Cundari, T. R. *J. Am. Chem. Soc.* **1992**, *114*, 7879−7888.
(31) Cundari, T. R.; Gordon, M. S. *J. Am. Chem. Soc.* **1993**, *115*, 4210−4217.
(32) Cundari, T. R.; Morse, J. M. *Chem. Mater.* **1996**, *8*, 189−196.
(33) Cundari, T. R.; Sommerer, S. O. *Chem. Vapor Depos.* **1997**, *3*, 183−192.
(34) Fix, R.; Gordon, R. G.; Hoffman, D. M. *Chem. Mater.* **1993**, *5*, 614−619.
(35) Frisch, M. J.; Trucks, G. W.; Schlegel, H. B.; Scuseria, G. E.; Robb, M. A.; Cheeseman, J. R.; Zakrzewski, V. G.; Montgomery, J. A.; Stratmann, R. E.; Burant, J. C.; Dapprich, S.; Millam, J. M.; Daniels, A. D.; Kudin, K. N.; Strain, M. C.; Farkas, O.; Tomasi, J.; Barone, V.; Cossi, M.; Cammi, R.; Mennucci, B.; Pomelli, C.; Adamo, C.; Clifford, S.; Ochterski, J.; Petersson, G. A.; Ayala, P. Y.; Cui, Q.; Morokuma, K.; Malick, D. K.; Rabuck, A. D.; Raghavachari, K.; Foresman, J. B.; Cioslowski, J.; Ortiz, J. V.; Stefanov, B. B.; Liu, G.; Liashenko, A.; Piskorz, P.; Komaromi, I.; Gomperts, R.; Martin, R. L.; Fox, D. J.; Keith, T.; Al-Laham, M. A.; Peng, C. Y.; Nanayakkara, A.; Gonzalez, C.; Challacombe, M.; Gill, P. M. W.; Johnson, B. G.; Chen, W.; Wong, M. W.; Andres, J. L.; Head-Gordon, M.; Replogle, E. S.; Pople, J. A. *Gaussian 98*; Gaussian, Inc.: Pittsburgh, PA.
(36) Becke, A. D. *Phys. Rev. A* **1988**, *38*, 3098−3100.
(37) Becke, A. D. *J. Chem. Phys.* **1993**, *98*, 5648−5652.
(38) Lee, C.; Yang, W.; Parr, R. D. *Phys. Rev. B* **1988**, *37*, 785−789.
(39) Krishnan, R.; Binkley, J. S.; Seeger, R.; Pople, J. A. *J. Chem. Phys.* **1980**, *72*, 650.
(40) McLean, A. D.; Chandler, G. S. *J. Chem. Phys.* **1980**, *72*, 5639.
(41) Wachters, A. J. H. *J. Chem. Phys.* **1970**, *52*, 1033.
(42) Hay, J. P. *J. Chem. Phys.* **1977**, *66*, 4377.
(43) Raghavachari, K.; Trucks, G. W. *J. Chem. Phys.* **1989**, *91*, 1062.

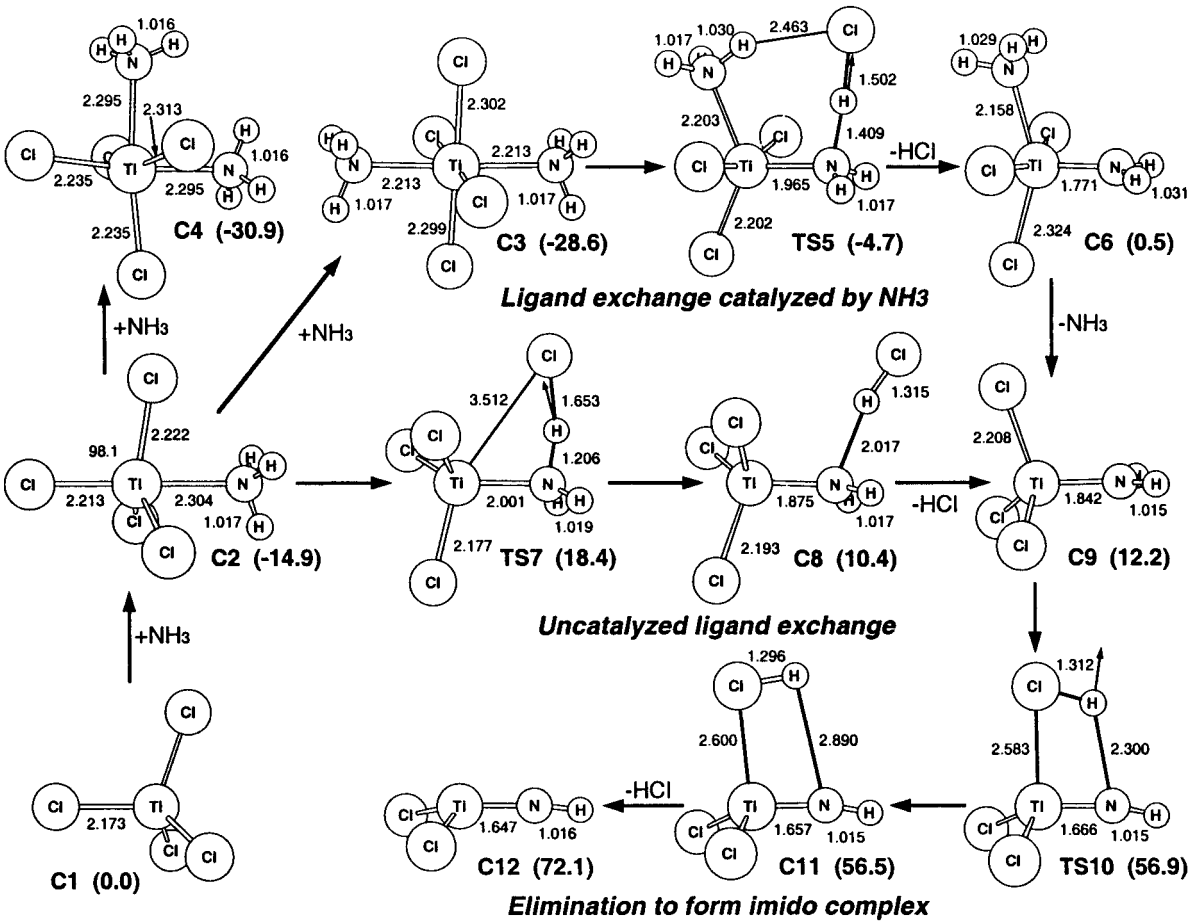

Figure 1. Structures on the reaction paths starting with $TiCl_4$, including molecules and complexes (denoted by C), and transition states with transition vectors (denoted by TS). Relative enthalpies at 0 K in kcal/mol are included in parentheses.

(For titanium, this corresponds to the 14s,9p,5d Wachters−Hay basis set[41−43] contracted to 9s,5p,3d and augmented with an f-type Gaussian shell with an exponent of 0.690.) Vibrational frequencies were computed at this level of theory and were used without scaling since the B3LYP frequencies agree quite well with experimental values for a wide range of second and third period compounds.[44] (However, the zero point energies were scaled by 0.9826, as was done in our previous paper.[18]) Thermal corrections to the energies were calculated by standard statistical thermodynamic methods[45] using the unscaled B3LYP frequencies. As in our previous work,[18] accurate energy differences were calculated using a modified G2 approach.[46−49] The B3LYP/6-311G(d) optimized geometries and vibrational frequencies were used instead of the MP2/6-31G(d) geometries and HF/6-31G(d) frequencies. Correlated energies were calculated by fourth-order Møller−Plesset perturbation theory[50,51] (MP4SDTQ, frozen core) and by quadratic configuration interaction with perturbative correction for triple excitations[52] (QCISD(T), frozen core) using the B3LYP geometries. The energy is computed in the usual fashion: the MP4/6-311G(d,p) energy is corrected for the effect of diffuse functions obtained at MP4/6-311+G(d,p), for the effect of higher polarization functions obtained at MP4/6-311G(2df,p), for the effect of electron correlation beyond fourth order obtained at QCISD(T)/6-311G(d,p), and for the inclusion of additional polarization functions at MP2/6-311+G(3df,2p). (For titanium, the 6-311+G(3df,2p) basis corresponds to the Wachters−Hay basis set[41,42] augmented with three sets of f functions and one set of g functions.) Higher level corrections (HLC) for deficiencies in the wave function are estimated empirically using the standard values.[46−49]

For larger structures with six and seven heavy atoms (i.e., systems involving $TiCl_4{\cdot}NH_3$, $TiCl_4{\cdot}(NH_3)_2$, and $Ti(NH_2)_4{\cdot}NH_3$), the G2 method was too costly, and energy differences were calculated at the B3LYP/6-311G(d), B3LYP/6-311+G(3df,2p), and MP2/6-311+G(3df,2p) levels of theory. When compared to the G2 level, B3LYP/6-311+G(3df,2p) performs significantly better than MP2/6-311+G(3df,2p) for heats of reaction [e.g., for $TiCl_3NH_2 \rightarrow TiCl_2NH + HCl$ (**C9** → **C12**): 59.9, 63.1,

(44) Scott, A. P.; Radom, L. *J. Phys. Chem.* **1996**, *100*, 16502−16513.
(45) McQuarrie, D. A. *Statistical Thermodynamics*; University Science Books: Mill Valley, CA, 1973.
(46) Curtiss, L. A.; Raghavachari, K.; Trucks, G. W.; Pople, J. A. *J. Chem. Phys.* **1991**, *94*, 7221−7230.
(47) Curtiss, L. A.; Carpenter, J. E.; Raghavachari, K.; Pople, J. A. *J. Chem. Phys.* **1992**, *96*, 9030−9034.
(48) Curtiss, L. A.; Raghavachari, K.; Pople, J. A. *J. Chem. Phys.* **1993**, *98*, 1293−1298.
(49) Raghavachari, K.; Curtiss, L. A. In *Modern Electronic Structure Theory*; Yarkony, D. R., Ed.; World Scientific Publishing: River Edge, NJ, 1995; p 459.
(50) Cremer, D. In *Encyclopedia of Computational Chemistry*; Schleyer, P. v. R., Allinger, N. L., Clark, T., Gasteiger, J., Kollman, P. A., Schaefer III, H. F., Schreiner, P. R., Eds.; Wiley: Chichester, 1998.
(51) Møller, C.; Plesset, M. S. *Phys. Rev.* **1934**, *46*, 618.
(52) Pople, J. A.; Head-Gordon, M.; Raghavachari, K. *J. Chem. Phys.* **1987**, *87*, 5968.

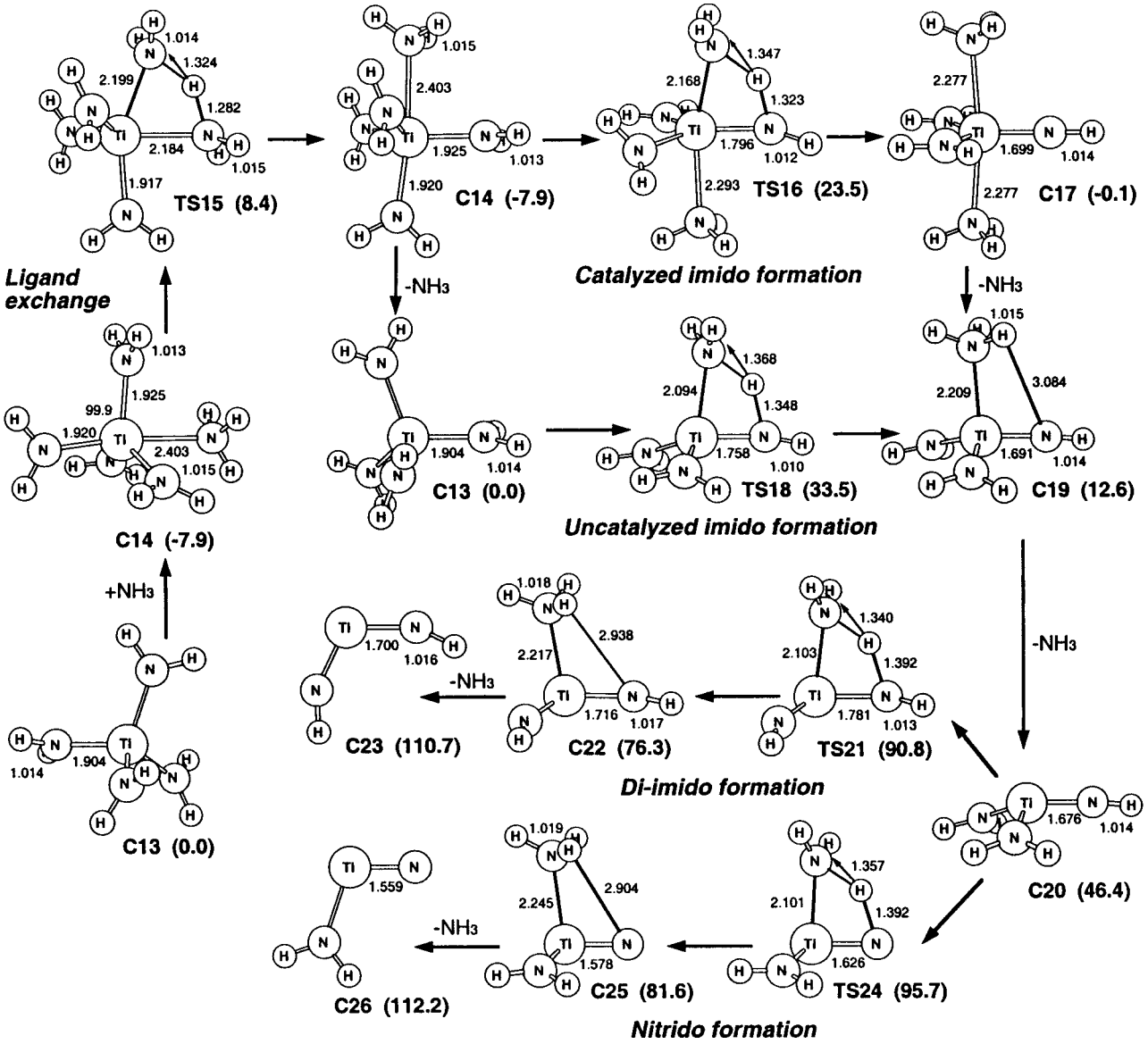

Figure 2. Structures on the reaction paths starting with $Ti(NH_2)_4$, including molecules and complexes (denoted by C), and transition states with transition vectors (denoted by TS). Relative enthalpies at 0 K in kcal/mol are included in parentheses.

and 52.0 kcal/mol for G2, B3LYP, and MP2, respectively; for $Ti(NH_2)_4 \rightarrow Ti(NH_2)_2NH + NH_3$ (**C13** → **C20**): 46.4, 43.8, and 35.7 kcal/mol for G2, B3LYP, and MP2, respectively]. Similarly, barrier heights at the B3LYP/6-311+G(3df,2p) level compare better with the G2 results [e.g., for $TiCl_3NH_2 \rightarrow TiCl_2NH + HCl$ (**C9** → **TS10**): 44.7, 50.7, and 36.0 kcal/mol for G2, B3LYP, and MP2, respectively; for $Ti(NH_2)_4 \rightarrow Ti(NH_2)_2NH + NH_3$ (**C13** → **TS18**): 35.5, 34.9, and 29.6 kcal/mol for G2, B3LYP, and MP2, respectively]. Thus, the barriers for $TiCl_4 \cdot NH_3 \rightarrow TiCl_3NH_2 \cdot NH_3 + HCl$ (**C2** → **TS7**) and $Ti(NH_2)_4 \cdot NH_3 \rightarrow Ti(NH_2)_3NH \cdot NH_3 + NH_3$ (**C14** → **TS15**) were calculated at the B3LYP/6-311+G(3df,2p) level.

Unfortunately, B3LYP/6-311+G(3df,2p) underestimates NH_3 binding energies by 6−8 kcal/mol. Similar trends were observed by Frenking and co-workers.[24] The MP2/6-311+G(3df,2p) and B3LYP/6-311G(d) results are in better agreement with G2 [e.g., for $Ti(NH_2)_2NH \cdot NH_3$ (**C20** → **C19**): 33.8, 33.9, 31.3, and 26.9 kcal/mol for G2, MP2/6-311+G(3df,2p), B3LYP/6-311G(d), and B3LYP/6-311+G(3df,2p), respectively]. Therefore, the MP2/6-311+G(3df,2p) values have been used for the NH_3 complexation energies for $TiCl_4 \cdot NH_3$ (**C1** → **C2**), $TiCl_3NH_2 \cdot NH_3$ (**C9** → **C8**), and $Ti(NH_2)_4 \cdot NH_3$ (**C13** → **C14**).

For the seven heavy atom systems, the 6-311+G(3df,-2p) basis was too costly. The energy differences were calculated at B3LYP/6-311G(d), since this level of theory provided satisfactory NH_3 binding energies and barrier heights when compared to the G2 values. Specifically, the energetics for **C2** → **C4**, **C2** → **C3** → **TS5** → **C6** and **C13** → **C14** → **TS16** and **C19** → **C17** were calculated at B3LYP/6-311G(d).

Results and Discussion

Structures derived from reaction of $TiCl_4$ with NH_3 are found in Figure 1; relative energies are plotted in Figure 3. Structures derived from reaction of $Ti(NH_2)_4$ with NH_3 are found in Figure 2; relative energies are plotted in Figure 4. Transition-state structures are labeled with TS and complexes representing minima are labeled with C. Computed enthalpies, entropies, and free energies are listed in Table 1.

1. Complexation of Ammonia with Ti(IV) Compounds. The initial gas-phase reactions for processes

Table 1. Heats of Formation, Absolute Entropies, Relative Enthalpies, and Relative Free Energies

	structure	$\Delta H_{f,298}$[a] (kcal/mol)	entropy[b] (cal/(mol K))	rel enthalpy[c] (kcal/mol)	rel free energy[d] (kcal/mol)
C1	$TiCl_4$	−182.4	83.9	0.0	0.0−0.0
C2	$TiCl_4{\cdot}NH_3$	−198.1	99.8	−15.7	24.7−15.2
C3	*cis*-$TiCl_4{\cdot}(NH_3)_2$	−214.9	112.2	−32.5	55.5−97.6
C4	*trans*-$TiCl_4{\cdot}(NH_3)_2$	−212.3	121.3	−29.9	49.6−95.1
TS5	$TiCl_3NH_2NH_3HCl$	−189.1	109.8	−6.7	83.7−64.6
C6	$TiCl_3NH_2{\cdot}NH_3$	−182.9	104.3	−0.5	38.3−28.8
TS7	$TiCl_3NH_2HCl$	−165.0	101.0	17.4	60.0−50.5
C8	$TiCl_3NH_2{\cdot}HCl$	−172.2	109.9	10.8	42.7−33.2
C9	$TiCl_3NH_2$	−169.9	93.4	12.5	0.9−0.9
TS10	$TiCl_2NHHCl$	−125.2	92.3	57.2	40.4−40.4
C11	$TiCl_2NH{\cdot}HCl$	−125.2	95.8	57.2	43.1−43.1
C12	$TiCl_2NH$	−109.3	81.0	73.1	12.8−22.3
C13	$Ti(NH_2)_4$	−66.3	93.0	0.0	0.0
C14	$Ti(NH_2)_4{\cdot}NH_3$	−75.0	104.4	−8.7	14.8
TS15	$Ti(NH_2)_4NH_3$	−59.2	102.8	7.1	30.3
TS16	$Ti(NH_2)_2NH(NH_3)_2$	−43.9	103.7	22.4	45.4
C17	$Ti(NH_2)_2NH{\cdot}(NH_3)_2$	−66.7	108.9	−0.4	23.8
TS18	$Ti(NH_2)_2NHNH_3$	−33.3	90.0	33.0	35.4
C19	$Ti(NH_2)_2NH{\cdot}NH_3$	−53.9	92.7	12.4	17.6
C20	$Ti(NH_2)_2NH$	−19.4	79.5	46.9	25.6
TS21	$Ti(NH)_2NH_3$	24.3	75.5	90.6	70.0
C22	$Ti(NH)_2{\cdot}NH_3$	10.2	78.9	76.5	57.5
C23	$Ti(NH)_2$	45.3	64.1	111.6	69.9
TS24	$Ti(NH_2)NNH_3$	29.3	76.5	95.6	74.8
C25	$Ti(NH_2)N{\cdot}NH_3$	15.7	80.6	82.0	62.8
C26	$Ti(NH_2)N$	46.9	66.1	113.2	70.2

[a] Heats of formation at 298.15 K and 1 atm, computed using the relative enthalpies for **C1**−**C26**, the experimental $\Delta H_{f,298}$ for $TiCl_4$ (−182.4 kcal/mol) and NH_3 (−11.0 kcal/mol), calculated $\Delta H_{f,298}$ for HCl (−22.4 kcal/mol), and the calculated enthalpy for $TiCl_4 + 4NH_3 \rightarrow Ti(NH_2)_4 + 4HCl$ (70.5 kcal/mol). [b] Absolute entropies at 298.15 K and 1 atm. [c] Enthalpies relative to **C1** or **C13** at 298.15 K and 1 atm; **C1** → **C9** → **TS10** → **C11** → **C12** and **C13** → **C20** → **TS21** → **C22** → **C23**, **C20** → **TS24** → **C25** → **C26** calculated at G2; **C1** → **C2**, **C8** → **C9** and **C13** → **C14** at MP2/6-311+G(3df,2p); **C2** → **TS7**, **C14** → **TS15** at B3LYP/6-311+G(3df,2p); **C1** → **C4**, **C1** → **C3** → **TS5** → **C6** and **C13** → **C14** → **TS16** → **C17** at B3LYP/6-311G(d). [d] Free energies relative to **C1** or **C13** at CVD conditions (for **C1**−**C12** conditions are 903.15 K and 0.1−20 Torr; for **C13**−**C26** conditions are 523.15 K and 20 Torr).

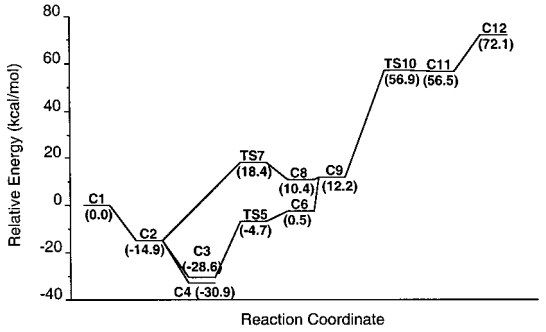

Figure 3. Energy profile for reaction paths starting with $TiCl_4$. Relative enthalpies at 0 K in kcal/mol are included in parentheses.

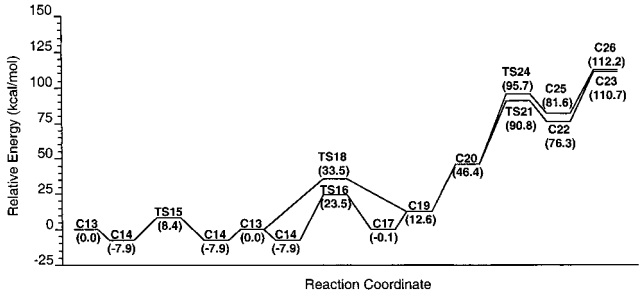

Figure 4. Energy profile for reaction paths starting with $Ti(NH_2)_4$. Relative enthalpies at 0 K in kcal/mol are included in parentheses.

1 and 2 appear to be the formation of complexes between $TiCl_4$ (**C1**) or $Ti(NR_2)_4$ (**C13**) and NH_3. The formation of the $TiCl_4{\cdot}NH_3$ complex (**C2**) yields a trigonal-bipyramidal C_{3v} structure, with NH_3 occupying an axial position with respect to the Cl atoms. The Ti−Cl bond lengths increase from 2.173 Å in $TiCl_4$ to 2.222 and 2.213 Å for equatorial and axial bonds, respectively, in $TiCl_4{\cdot}NH_3$. As expected for a dative bond, the Ti−NH_3 bond length, 2.304 Å, is considerably longer than in $Ti(NH_2)_4$, 1.904 Å. (Optimization at B3LYP/6-311+G(3df,2p) does not change these results significantly.) Similar geometries and trends were observed by Frenking and co-workers.[24] Inspection of the molecular orbitals reveals that this bond is composed of the nitrogen p-orbital overlapping with the titanium d_{z^2}-orbital.

For the amido species, a model compound, $Ti(NH_2)_4$, was studied instead of $Ti(NR_2)_4$ in order to keep the cost of the calculations manageable. The formation of the $Ti(NH_2)_4{\cdot}NH_3$ complex (**C14**) from $Ti(NH_2)_4$ and NH_3 results in a trigonal-bipyramidal structure similar to $TiCl_4{\cdot}NH_3$, but with C_s instead of C_{3v} symmetry (the orientation of the hydrogens in the amido ligands lowers the symmetry) and with the NH_3 group occupying an axial position. The amido Ti−N bond lengths increase from 1.904 Å in $Ti(NH_2)_4$ to 1.937 and 1.925 Å for the equatorial and 1.920 Å for the axial Ti−NH_2 bonds in $Ti(NH_2)_4{\cdot}NH_3$. The Ti−NH_3 bond length, 2.403 Å, is longer than the corresponding bond length in $TiCl_4{\cdot}NH_3$, in agreement with earlier calculations.[24]

It is difficult to obtain an accurate estimate of the binding energies of $TiX_4{\cdot}NH_3$ because these complexes are too large to compute with the G2 method. Complexation energies calculated at the B3LYP/6-311G(d), B3LYP/6-311+G(3df,2p), and MP2/6-311+G(3df,2p) levels of theory are 16.9, 9.2, and 14.2 kcal/mol for $TiCl_4{\cdot}NH_3$ and 6.3, 1.2, and 7.9 kcal/mol for $Ti(NH_2)_4{\cdot}NH_3$, respectively. For $Ti(NH_2)_2NH{\cdot}NH_3$, the MP2/6-311+G-

(3df,2p) and B3LYP/6-311G(d) results agree best with the G2 values (see the Methods section); hence, they should also be the most reliable for $TiX_4 \cdot NH_3$. The present calculations, as well as those of Frenking and co-workers,[24] consistently predict that the binding energy for $Ti(NH_2)_4 \cdot NH_3$ is 8−10 kcal/mol smaller than for $TiCl_4 \cdot NH_3$, which is in accord with the longer Ti−NH_3 bond. Inspection of the orbital energies of the $TiCl_4$ and $Ti(NH_2)_4$ precursors shows that the d-orbitals are much lower in $TiCl_4$ (−0.43 au vs −0.33 au), which leads to stronger binding of the NH_3 ligand and a shorter Ti−NH_3 bond. This is also supported by the larger charge transfer from nitrogen to titanium computed for $TiCl_4 \cdot NH_3$ compared to that for $Ti(NH_2)_4 \cdot NH_3$.

For $TiCl_4$, the calculated a_1 and t_2 Ti−Cl stretching frequencies, 389 and 501 cm^{-1}, agree very well with the observed frequencies,[53] 388 and 499 cm^{-1}. In the $TiCl_4 \cdot NH_3$ complex, the computed Ti−Cl modes are shifted to lower frequencies, 370, 441, and 451 cm^{-1} for the symmetric equatorial, axial, and asymmetric equatorial stretches, respectively. The observed modes at 440 and 456 cm^{-1} correspond to the axial and asymmetric equatorial Ti−Cl stretches; the symmetric equatorial stretch is below the 400 cm^{-1} limit of the spectrometer.[21] Other diagnostic frequencies include the NH_3 rock, 683 cm^{-1} calcd vs 624 cm^{-1} exp, and the NH_3 symmetric deformation, 1329 cm^{-1} calcd vs 1198 cm^{-1} exp.

There are no experimental vibrational frequencies published for $Ti(NH_2)_4 \cdot NH_3$. The calculated Ti−NH_2 stretching frequencies in $Ti(NH_2)_4 \cdot NH_3$ are 629, 692, 715, and 719 cm^{-1}, compared to 648 and 731 cm^{-1} calculated for the a_1 and t_2 modes in $Ti(NH_2)_4$. Other calculated diagnostic frequencies include 513 and 522 cm^{-1} for the NH_3 rock and 1186 cm^{-1} for the NH_3 symmetric deformation.

$TiCl_4 \cdot (NH_3)_2$ has been used as a single source precursor for deposition of Ti−N thin films.[23] Mixing of $TiCl_4$ and excess NH_3 in solution[23] or in the gas phase[54] leads to a yellow solid, which can be sublimed at 120 °C, [23] decomposes above 250 °C,[55] and forms titanium nitride above 500 °C.[23,54] This is consistent with the NH_3 binding energy of ca. 30 kcal/mol computed at the B3LYP/6-311G(d) level. The cis isomer is calculated to be 2 kcal/mol more stable than the trans isomer, in agreement with previous calculations[24] and the experimental preference for cis isomers in $TiCl_4 \cdot A_2$ in the absence of steric crowding.[56] The *cis*-$TiCl_4 \cdot (NH_3)_2$ isomer (**C4**) has C_2 symmetry, with the rotation axis bisecting the N−Ti−N angle. The lengths for Ti−N and Ti−Cl bonds that are in the same plane are similar to those in the $TiCl_4 \cdot NH_3$ complex; however, the Ti−Cl bonds perpendicular to this plane are elongated by ca. 0.1 Å. The *trans*-$TiCl_4 \cdot (NH_3)_2$ isomer (**C3**) is very close to C_s symmetry, but rotation of the NH_3 groups by 12.5° breaks the symmetry. Compared to $TiCl_4 \cdot NH_3$, the Ti−Cl bonds are 0.08 Å longer and the Ti−N bonds are 0.09 Å shorter. The geometric variations in the cis and trans isomers can be rationalized in terms of the trans influence.[57] In the present case, this is manifested by a lengthening of the bond trans to each Cl ligand. Similar trends have been seen experimentally in $TiCl_4 \cdot (THF)_2$, where crystal structures are available for both isomers.[14]

The experimental vibrational data for $TiCl_4 \cdot (NH_3)_2$[23] are less detailed than for $TiCl_4 \cdot NH_3$. The calculated Ti−Cl stretches are 360, 370, 414, and 416 cm^{-1} for cis and 371, 371, 382, and 428 cm^{-1} for trans. The band observed[23] at 421 cm^{-1} could belong to either the cis or the trans isomer (400 cm^{-1} was the lower limit of the spectrometer). The calculated NH_3 rocking modes (613, 679, 685, 722 cm^{-1} for cis, 676, 683, 708, 714 cm^{-1} for trans) correspond to the observed NH_3 rocking mode at 678 cm^{-1}. The NH_3 symmetric deformations are calculated at 1312 and 1330 cm^{-1} for cis, and 1317 and 1322 cm^{-1} for trans, compared to the observed frequencies at 1238 and 1255 cm^{-1}. The calculated splitting for the cis isomer is in much better agreement with the experimental splitting, suggesting that the observed structure is the cis isomer.

2. Ligand Exchange Reactions. For atmospheric pressure CVD of titanium nitride from $TiCl_4$ or $Ti(NR_2)_4$ and NH_3, one of the rate-limiting steps may be the formation of amido complexes in the gas phase. The stability of the $TiCl_4 \cdot NH_3$ (**C2**) and $Ti(NH_2)_4 \cdot NH_3$ (**C14**) complexes described above suggests that this reaction occurs via these intermediate complexes. The first step in this process is one of the following reactions:

$$TiCl_4 + NH_3 \rightarrow TiCl_3NH_2 + HCl \quad (3)$$

$$Ti(NR_2)_4 + N'H_3 \rightarrow Ti(NR_2)_3N'H_2 + HNR_2 \quad (4)$$

An analogous step may occur on the surface for low-pressure CVD. Subsequent replacements of Cl or NR_2 by NH_2 in the gas phase or on the surface proceed in a similar fashion.[24]

The structures along the $TiCl_4 + NH_3 \rightarrow TiCl_3NH_2 + HCl$ reaction path are labeled as uncatalyzed ligand exchange in the center of Figure 1. The reaction is calculated to be endothermic by 12.2 kcal/mol at the G2 level of theory. The transition state (**TS7**) can be characterized as late, which is consistent with an endothermic reaction. The Ti−Cl bond is nearly broken (elongated from 2.222 Å in the complex to 3.512 Å in the transition state), and the H−Cl bond is partially formed (1.653 vs 1.275 Å in HCl). The N−H bond is not yet broken (1.206 Å in the transition state), and the Ti−N bond length (2.001 Å) is approximately halfway between reactants and products. The transition state is ca. 33 kcal/mol above the complex at the B3LYP/6-311+G(3df,2p) level of theory, as illustrated in Figure 3. Frenking and co-workers[24] found similar structures, but their barriers were somewhat higher because smaller basis sets were used. On the product side of the transition state, there is a weakly bound complex (**C8**) with a hydrogen bond between the hydrogen of HCl and the nitrogen of $TiCl_3NH_2$. The binding energy, 1.8 kcal/mol, is significantly less than $H_3N \cdot HCl$ (11.8 kcal/mol) because the lone pair of the amido ligand is involved in bonding to the titanium. Nevertheless, the H−Cl bond shows the characteristic lengthening due to hydrogen

(53) Hawkins, N. M.; Carpenter, D. R. *J. Chem. Phys.* **1955**, *23*, 1700.
(54) Hojo, J.; Kato, A. *Yogyo-Kyokai-Shi* **1981**, *89*, 277.
(55) Fowles, G. W. A.; Pollard, F. H. *J. Chem. Soc.* **1953**, 2588.
(56) Guzei, I. A.; Winter, C. H. *Inorg. Chem.* **1997**, *36*, 4415−4420.
(57) Cotton, F. A.; Wilkinson, G. *Advanced Inorganic Chemistry*; Wiley: New York, 1992.

bonding (1.315 Å in $TiCl_3NH_2$·HCl and 1.382 Å in H_3N·HCl vs 1.275 Å in HCl).

For titanium nitride CVD from $Ti(NR_2)_4$ and NH_3, the amido ligand exchange (transamination) reaction, $Ti(NR_2)_4 + NH_3 \rightarrow Ti(NR_2)_3NH_2 + HNR_2$, appears to be the rate-determining step when the process is not mass transport limited.[28] Titanium amido complexes undergo transamination reactions readily in solution[58] and in the gas phase.[4,20,26−28] The kinetics for $Ti(NR_2)_4 + NH_3 \rightarrow Ti(NR_2)_3NH_2 + HNR_2$ have been studied experimentally[26−28] and yield activation energies of E_a = 8 kcal/mol for R = Me and 12 kcal/mol for R = Et. Mechanistic studies[26−28] have found that the addition of HNR_2 reduces the rate of film growth by competing with NH_3 in the ligand exchange, thereby showing that the transamination reactions involved in the CVD process are reversible.

As illustrated in Figure 2, the simplest transamination reaction with R = H is examined in the present work. This is a thermoneutral, identity reaction that proceeds through a $Ti(NH_2)_4$·NH_3 complex and involves the transfer of a single H atom from the NH_3 group to an NH_2 ligand, yielding a product structure which is identical to the initial reactant structure. The calculated transition state is ca. 16 kcal/mol above the $Ti(NH_2)_4$·NH_3 complex at the B3LYP/6-311+G(3df,2p) level of theory and, as expected, has a geometry midway between reactants and products. The Ti−NH_2 bond elongates from 1.925 Å in the complex to 2.199 Å in the transition state, the Ti−NH_3 bond shortens from 2.403 Å in the complex to 2.184 Å in the transition state, and the hydrogen is nearly equidistant from the two nitrogens. (The presence of the other three amido groups prevents the transition state from being totally symmetric.)

Because of the stability of the complexes between $TiCl_4$ and two NH_3 molecules, ligand exchange could proceed via a six-coordinate intermediate by the following reaction:

$$TiCl_4 + 2NH_3 \rightarrow TiCl_4\cdot(NH_3)_2 \rightarrow TiCl_3NH_2\cdot NH_3 + HCl \quad (5)$$

The structures along this reaction path for elimination of HCl from *trans*-$TiCl_4$·$(NH_3)_2$ are labeled as ligand exchange catalyzed by NH_3 in Figure 1. The presence of the second NH_3 ligand reduces the barrier height by 12.4 kcal/mol compared to the case of the $TiCl_4$·NH_3 transition state where both are calculated at B3LYP/6-311+G(3df,2p). Frenking and co-workers[24] did not observe as much stabilization because the conformation of their transition state did not facilitate hydrogen bonding between NH_3 and Cl. This transition state (**TS5**) lies ca. 24 kcal/mol above the *trans*-$TiCl_4$·$(NH_3)_2$ complex at the B3LYP/6-311G(d) level of theory and occurs even later along the reaction path than the $TiCl_4$·NH_3 transition state (**TS7**). The Ti−Cl bond is longer (3.833 vs 3.512 Å) and the H−Cl bond is shorter (1.502 vs 1.653 Å) than in the $TiCl_4$·NH_3 transition state. The N−H bond is nearly broken (1.409 Å in the transition state), which causes the Ti−N bond length to decrease to 1.965 Å. There is likely to be a weakly bound complex on the product side of this reaction similar to that found for the $TiCl_4$·NH_3 reaction, but this part of the reaction scheme was not pursued in this investigation.

3. Elimination Reactions Forming Imido Complexes. The amido compounds formed in the ligand exchange reactions can eliminate HCl or NH_3 to produce more reactive imido complexes:

$$TiCl_3NH_2 \rightarrow TiCl_2NH + HCl \quad (6)$$

$$Ti(NH_2)_4 \rightarrow Ti(NH_2)_2NH + NH_3 \quad (7)$$

The elimination of HCl from $TiCl_3NH_2$ (**C9**) is calculated to be endothermic by 59.9 kcal/mol at the G2 level of theory and has a transition state (**TS10**) of C_s symmetry lying 44.7 kcal/mol above the reactants. Using a lower level of theory, Cundari and Gordon have found similar energetics for HCl elimination from the model compound $TiClH_2NH_2$[31] but found a transition state considerably earlier along the reaction path. In **TS10** the N−H bond has completely dissociated (2.30 Å in the $TiCl_3NH_2$ TS vs 1.72 Å in the $TiClH_2NH_2$ TS[31]), and the H−Cl bond is fully formed (1.31 Å in the $TiCl_3$-NH_2 TS vs 1.39 Å in the $TiClH_2NH_2$ TS[31] vs 1.28 Å in HCl). The transition state is followed by an adduct (**C11**) between the imido complex and HCl. This adduct is bound by less than 1 kcal/mol relative to the transition state, but by ca. 15.6 kcal/mol relative to the dissociated products, indicating a fairly strong donor−acceptor interaction between Ti and Cl. The Ti=NH stretching vibrational frequency of the product, 1055 cm^{-1},[18] is a potential probe for this imido intermediate.

Chemical vapor deposition from $Ti(NR_2)_4$ and NH_3 starts with a transamination reaction to form $Ti(NR_2)_3$-NH_2. This system has been modeled with $Ti(NH_2)_4$ instead of $Ti(NR_2)_3NH_2$. $Ti(NH_2)_4$ can also be formed from $TiCl_4$ and NH_3 by exchanging all four Cl's for amido ligands. The elimination of NH_3 from $Ti(NH_2)_4$ proceeds by transferring a hydrogen atom from one amido group to another, followed by dissociation of NH_3. The reaction is calculated to be endothermic by 46.4 kcal/mol, and the transition state (**TS18**) lies 33.5 kcal/mol above the reactants at the G2 level. The transition state has C_s symmetry and occurs significantly earlier along the reaction path than HCl elimination from $TiCl_3NH_2$. The migrating hydrogen is almost equidistant between the two nitrogens (1.348 Å from the nitrogen it is leaving and 1.368 Å from the nitrogen it is approaching). One of the Ti−N bonds has elongated to 2.094 Å and another has shortened to 1.758 Å compared to the bond length of 1.904 Å in the reactant. Cundari et al.[31,32] have found very similar transition states for NH_3 elimination from the model compounds $TiH_2(NH_2)_2$ and $TiH_2(NHMe)NH_2$ using a more modest level of theory. There is a complex (**C19**) on the product side of the transition state that lies 20.9 kcal/mol below the transition state and 33.8 kcal/mol below the products. It is characterized by a fully formed Ti=NH double bond (1.691 Å) and a strong dative bond between Ti and NH_3 (2.209 Å). Diagnostic vibrations for this complex are 1248 cm^{-1} for the NH_3 symmetric deformation and 1008 cm^{-1} for the Ti=NH stretch. The latter mode is at 1030 cm^{-1} in the uncomplexed products.[18]

The formation of uncomplexed imido species from either $TiCl_3NH_2$ or $Ti(NH_2)_4$ is rather endothermic.

(58) Bradley, D. C.; Torrible, E. G. *Can. J. Chem.* **1963**, *41*, 134.

However, the calculations described above show that the imido compounds readily form complexes and that the binding to ammonia is significantly stronger than the binding to HCl. Since excess ammonia is used in low-temperature CVD from $Ti(NR_2)_4$,[11] complexation with NH_3 could assist the elimination reaction to form the imido species:

$$Ti(NH_2)_4 \cdot NH_3 \rightarrow Ti(NH_2)_2NH \cdot (NH_3)_2 \qquad (8)$$

Geometries of the transition state and complexes are labeled as catalyzed imido formation in Figure 2. The complexation energies were computed at the B3LYP/6-311G(d) level, since these structures are too large to calculate expediently by the G2 protocol. For the smaller $Ti(NH_2)_2NH \cdot NH_3$ complex (**C19**), the NH_3 binding energy computed at B3LYP/6-311G(d), 34.3 kcal/mol, is in good agreement with the G2 value, 33.8 kcal/mol. The reaction of the complexed species is more nearly thermoneutral, and the barrier is lowered by ca. 1 kcal/mol relative to $Ti(NH_2)_2NH \cdot NH_3$ but is reduced by ca. 9 kcal/mol relative to $Ti(NH_2)_2NH + NH_3$. In the transition state (**TS16**), the migrating hydrogen remains nearly equidistant from the two nitrogens, but complexation makes the titanium less pyramidal and the inequivalent amido ligands break the symmetry. In the imido species complexed with two ammonias (**C17**), the titanium is planar, and the Ti═NH and Ti−NH_3 bonds are elongated only slightly when compared to the complex with one ammonia. The small changes in the geometry are in keeping with the fact that the binding energy for the second ammonia, 12.7 kcal/mol, is much smaller than for the first ammonia, 33.8 kcal/mol. Characteristic frequencies are 1196 and 1201 cm^{-1} for the NH_3 asymmetric and symmetric deformations and 990 cm^{-1} for the Ti═NH stretch, values slightly lower than for the complex with one ammonia.

4. Elimination of NH_3 from $Ti(NH_2)_2NH$. If the elimination of one NH_3 is possible, perhaps a second NH_3 can also be removed. There are two pathways to consider. Migration of the imido hydrogen of $Ti(NH_2)_2NH$ (**C20**) would yield a nitrido product, $Ti(NH_2)N$ (**C26**), and ammonia:

$$Ti(NH_2)_2NH \rightarrow Ti(NH_2)N + NH_3 \qquad (9)$$

Alternatively, removal of an amido hydrogen from $Ti(NH_2)_2NH$ results in a diimido species (**C23**) plus ammonia:

$$Ti(NH_2)_2NH \rightarrow Ti(NH)_2 + NH_3 \qquad (10)$$

The reactions are calculated to be nearly equally endothermic at the G2 level, 65.8 and 64.3 kcal/mol for the formation of the nitrido and diimido species, respectively. The corresponding barriers are also similar, 49.3 and 44.4 kcal/mol, with the diimido being slightly lower. In both cases, the migrating hydrogen is approximately halfway between the two nitrogens, and the Ti−N distance for the departing nitrogen has increased from 1.92 Å in the reactants to 2.10 Å in the transition state. The product side complexes lie ca. 14 kcal/mol below the transition states and consist of an NH_3 forming a dative bond with Ti in the nitrido or diimido product. The Ti−NH_3 bond lengths are comparable, 2.22−2.25 Å, and the nitrido or diimido fragments have geometries very similar to the products. Characteristic vibrational frequencies for the products include the Ti−NH_2 stretch, 677 cm^{-1}, and Ti−N stretch, 1153 cm^{-1}, for the nitrido species and asymmetric Ti═NH stretch, 971 cm^{-1}, and symmetric Ti═NH stretch, 988 cm^{-1}, for the diimido species.

Conclusions

The discussion above has focused on characterizing the gas-phase reaction paths for titanium nitride chemical vapor deposition in terms of computed structures, enthalpies, and vibrational frequencies of the most probable intermediates and transition states. Experimentally, these CVD reactions are carried out at high temperatures and low partial pressures. To interpret our calculated results for the experimental conditions, we need to examine the free energies. The heats of formation, absolute entropies, relative enthalpies, and relative free energies for the structures studied in this paper are collected in Table 1.

Ligand exchange reactions starting with the $TiCl_4$ precursor are either endothermic or slightly exothermic. For ligand exchange with a single NH_3 group the reaction is calculated to be endothermic by 12.2 kcal/mol, but $\Delta G_{rxn} = 0.9$ kcal/mol at 0.1 Torr and 630 °C. This suggests that ligand exchange through complexation with a single NH_3 group is thermodynamically feasible at CVD conditions. The transition state barrier is lowered by 9.4 kcal/mol, and the reaction becomes nearly thermoneutral ($\Delta H_{rxn} = -2.0$ kcal/mol) for ligand exchange when a second NH_3 group is added to the complex and $TiCl_3NH_2 \cdot NH_3$ is formed, suggesting a catalyzed route to ligand exchange. However, calculations of the free energy reveal that $\Delta G_{rxn} = 38.3-28.8$ kcal/mol at 0.1−20 Torr and 630 °C, making this route much less favorable than the pathway involving complexation of a single NH_3.

Elimination reactions to form imido complexes are rather endothermic and have relatively high barriers at the G2 level. The direct elimination of HCl from $TiCl_3NH_2$ is calculated to have $\Delta G_{rxn} = 11.9$ kcal/mol at 0.1 Torr and 630 °C. Since elimination of NH_3 is less exothermic, CVD from $TiCl_4$ may involve multiple exchanges of NH_2 for Cl before the elimination step. Multiple ligand exchanges, in turn, may require efficient removal of HCl to shift the equilibrium appropriately.

CVD from $Ti(NR_2)_4$ is carried out at lower temperatures and higher partial pressures. Elimination of NH_3 from $Ti(NH_2)_4$ is calculated to have $\Delta G_{rxn} = 25.6$ kcal/mol at 20 Torr and 250 °C. However, if ammonia remains complexed to the imide, the reaction is more favorable with $\Delta G_{rxn} = 17.6$ kcal/mol. Complexation with one additional ammonia lowers the enthalpy of the reactants by 6.3 kcal/mol but raises the free energy by 14.8 kcal/mol. Complexation also decreases the enthalpy of the transition state and product side complex by 10.9 and 12.7 kcal/mol, respectively, but increases their free energy by 10.0 and 6.2 kcal/mol. Thus, complexation with additional ammonia does not facilitate the gas-phase reaction at 250 °C and 20 Torr. However, if complexation to a surface bound NH_2 group is stronger than to a free NH_3, the surface reaction could be more favorable than the gas-phase reaction.

The experimental kinetics indicates that the elimination reaction is slower than the transamination.[26−28] The present work is consistent with this observation since the calculated free energy barrier for the elimination $Ti(NH_2)_4 \rightarrow Ti(NH_2)_2NH{\cdot}NH_3$ is 5.1 kcal/mol higher than for the transamination of $Ti(NH_2)_4$ at 250 °C and 20 Torr. The free energy barriers for the formation of the diimido and nitrido complexes are about 10 kcal/mol higher than the barrier for the formation of the imido complex; hence, these reactions are less likely in the gas phase.

Acknowledgment. We gratefully acknowledge support from the National Science Foundation (CHE 98-74005) and from the National Computational Science Alliance under CHE980042N utilizing the NCSA HP/Convex Exemplar SPP-2000.

Supporting Information Available: Tables of total energies, Cartesian coordinates, and vibrational frequencies of the structures described in this work. This material is available free of charge via the Internet at http://pubs.acs.org.

CM000107L